Latex Modification Effects on the Mechanisms of Microcrack Propagation in Concrete Materials

PARVIZ SOROUSHIAN AND ATEF TLILI

Improvements in the matrix microstructure associated with latex modification of plain and steel-fiber-reinforced concrete materials are assessed. In particular, this study investigates the effects of latex modification of concrete matrix on the microcracking and failure mechanisms. In order to study the process of failure in concrete under increasing stress levels, microscopic investigations were performed on concrete cylinders preloaded to different compressive stress levels. The effects of latex modification of concrete matrix on the microcracking and failure mechanisms were also investigated. Five stress levels were selected. At each stress level, two thin slices, one longitudinal and the other transverse, were prepared and investigated for microcracking characteristics after special surface preparation. Through the use of an image analysis system, three different types of measurements were made: aggregate-interface (bond) crack length per unit area; matrix crack length per unit area; and microcrack orientation defined as the average crack inclinations with respect to the direction of loading. In plain concrete, microcracks were found to be present even before loading, because of factors such as differential shrinkage movements, settlements, and thermal strains between aggregates and cement paste. They appeared dominantly at the coarse aggregate-cement paste interfaces. At higher compressive stress levels, the propagation of microcracks extended from interfaces into the matrix. At peak compressive stress, microcracks had a tendency to interconnect and localize. Latex modification of concrete reduced the microcrack intensities at lower stress levels; this was particularly true for the aggregate-cement paste interface microcracks. Measurements on microcrack orientation revealed that the matrix microcracks were generally oriented less than 20 degrees from the longitudinal axis of the specimen (i.e., the direction of loading). At the aggregate-cement interface, the microcrack orientation was random.

Concrete materials suffer from microcracking at cement-aggregate interfaces, along fiber-matrix interfaces, or around the entrapped air voids, even before loading. Under increased loading, microcracks tend to grow and interconnect to form microcrack channels or get arrested by matrix constituents such as aggregates, steel fibers, and air voids.

Latex polymers in plain and steel-fiber-reinforced concrete (SFRC) reduce the microcracking damage under external loading because of their pore filling and superior interface zone bonding.

BACKGROUND

Under external loading, microcracks occur (or start to grow) at the cement-aggregate interfaces, around the entrapped air voids, or along the fiber-matrix interfaces. With increased loading, some microcracks grow and connect with each other to form large macrocracks, while some others are arrested by aggregates, air voids, or fibers. The propagation of microcracks leads to increased nonlinearity of the material before the peak load is reached.

For air-dried mortar and concrete, shrinkage-induced bond cracks around large aggregate particles appear before any loading (*1*) (see Figure 1). Under load, debonding and multiple cracking around sand grains and air voids are observed frequently (*1*), and this phenomenon seems to be more pronounced between adjacent sand grains than around isolated ones. In normal-weight concrete, the crack changes orientation when it encounters an aggregate by passing around it instead of crossing it (see Figure 2) (*1*). In concrete, the crack

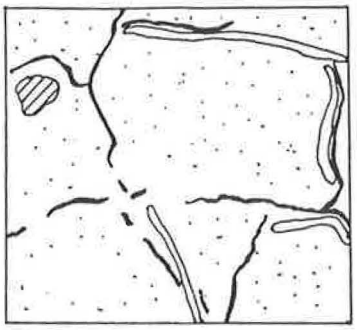

FIGURE 1 Bond crack before loading in air-dried mortar.

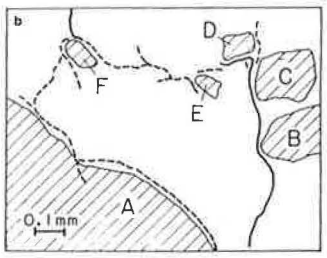

FIGURE 2 Shifting of crack direction after encountering aggregates (*1*).

Department of Civil and Environmental Engineering, Michigan State University, East Lansing, Mich. 48824.

pattern is more tortuous than in mortar (Figure 3) because concrete cracks must propagate around the densely spaced aggregate pieces as well as sand grains. The reorientation, branching, and multiple cracking associated with the interaction of microcracks with the encountered aggregate particles lead to the dissipation of a large amount of energy, which is beneficial to the material behavior under load.

When fibers are present in the matrix, the growth and interconnection of microcracks become a more energy-absorptive process and thus fibers enhance the prepeak behavior and the ultimate tensile strength of fiber-reinforced concrete.

Once a microcrack intersects a fiber at an angle, it generally interacts with the fiber in a manner that makes further propagation more energy absorptive (see Figure 4). The microcrack can advance beyond a steel fiber along its original path as shown in Figure 5a (20 percent of the time), by shifting as shown in Figure 5b (30 percent of the time), or by branching into multiple postfiber cracks as shown in Figure 5c (50 percent of the time). The microcrack encountering a fiber stays continuous, making the lateral shifts around the fibers, as can be clearly seen in the picture of the groove under a steel fiber that intersected microcracks in Figure 6.

Microcrack propagation at the fiber-matrix interface might take place at the interface itself, leading to the separation of matrix from the fiber by debonding (Figure 7a), or it might occur at a small distance (~20 μm) from the fiber and parallel to it by pseudodebonding (Figure 7b) that separates the body of the matrix from a thin layer of interface that remains attached to the fiber.

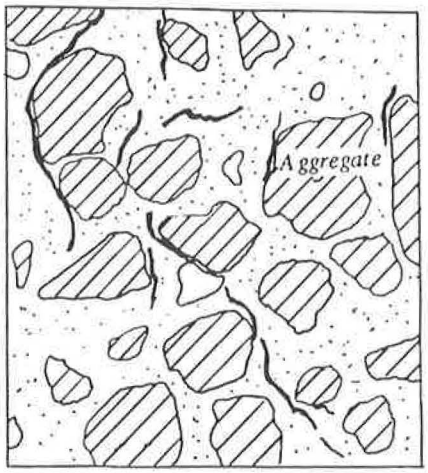

FIGURE 3 Tortuosity of cracking.

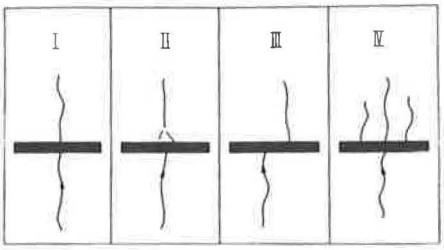

FIGURE 4 Cracking patterns observed at the intersection of a propagating crack and a fiber normal to its path (*1*).

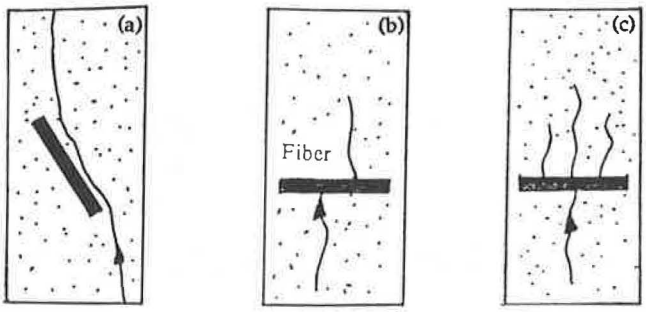

FIGURE 5 Illustrations of crack types (a) parallel running, (b) shifting, and (c) branching.

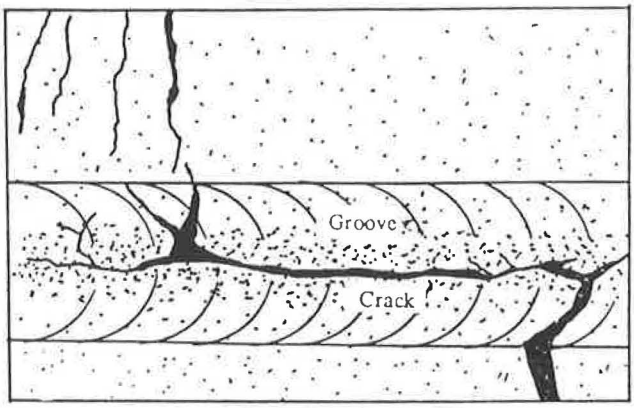

FIGURE 6 Continuous nature of shifted microcracks around a steel fiber.

With their microcrack-arresting action, fibers tend to increase the fracture energy and consequently the tensile strength of concrete. Fiber pull-out or rupture tends to dominate the postcracking progress of failure in SFRC under direct tension.

EXPERIMENTAL PROGRAM

For each one of the mixes presented in Table 1, 15 specimens were cast. The specimens were 75 mm (3 in.) in diameter and 150 mm (6 in.) long. They were moist-cured for 48 hr inside their molds while being covered with a wet burlap and a plastic sheet, and then air-cured until the test age of 28 days. Three specimens out of each group of 15 were tested under compression until failure, with stresses and strains monitored throughout the test. On the basis of the average compressive strength (f'_c) obtained from these three tests for each mix, five stress levels were selected and two specimens of the same mix were loaded to each predetermined stress level and then unloaded. The five stress levels considered in this study were 0.00 f'_c, 0.30 f'_c (prepeak), 0.80 f'_c (prepeak), 1.00 f'_c (peak), and 0.90 f'_c (postpeak).

After each specimen was covered with a thin layer of epoxy, the specimen was encased (i.e., circumscribed) in a fibrous mortar mount 100 mm (4 in.) in diameter. This mount was

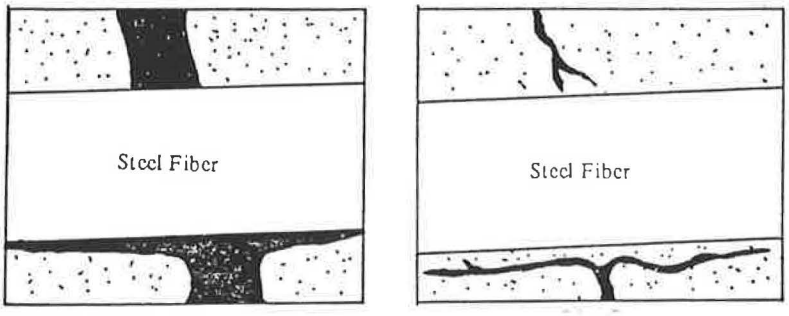

FIGURE 7 Microcrack propagation at the steel fiber–cement interface, (a) debonding, and (b) pseudo-debonding.

necessary to maintain the integrity of specimens (especially those loaded to large strains) during handling and slicing for microstructural investigations. The specimens were then sectioned, one transversely and one longitudinally, to slices 13 mm (0.5 in.) thick that were cut from the center of the specimen using a diamond saw (see Figure 8).

The slices were then washed in a jet of water and allowed to dry in the laboratory for 24 hr. They were then stained with black indian ink, grouped with silicon carbide on rotating laps over a sequence of five grit sizes: #180, #240, #320, #400, and #600. These specimen preparation steps help distinguish the microcracks under the microscope. Figure 9 shows a view of the longitudinal and transverse slices after being prepared for microstructural studies.

The slices were examined for microcracking characteristics using an image analysis system of typical magnification 25×. The cracks at the prepared faces of the slices were visible as black lines. The microstructural studies were conducted after dividing the surface area of the slice to be viewed under the microscope into about thirty 13- × 13-mm (0.5- by 0.5-in.) squares, each to be viewed as a separate field of measurement (see Figure 9).

Once subdivided, the slices were viewed through a microscope connected to the image analysis system. For each field of view on the microscope (which covers a 4- × 3-mm area within each 13- × 13-mm square of the mesh), the following three measurements were performed:

1. The intensity of bond cracks at aggregate- and fiber-cement interfaces (as shown in Figure 10) with intensity defined as the total crack length per unit area;
2. The intensity of matrix cracks (both aggregate interface and matrix cracks are shown in Figure 11); and
3. Microcrack orientations defined as the average inclination of cracks with respect to the direction of loading (performed on the longitudinal slices only).

Measurements on microcrack intensity reveal information on the process of failure in concrete materials under increasing stress levels, as influenced by the presence of steel fibers and latex polymers. Inclinations of microcracks provide indications of the nature of failure mechanism under compression.

EXPERIMENTAL RESULTS

Results of microstructural studies on the process of microcrack propagation and failure under compressive stresses in plain, latex-modified concrete (LMC) and latex-modified steel-

TABLE 1 SELECTED-MIX PROPORTIONS FOR EXPERIMENTAL WORK FOR SAND-CEMENT AND GRAVEL-CEMENT RATIOS OF 2.5 AND 1.5, BY WEIGHT, RESPECTIVELY

V_f (%)	Styrene Butadiene L/c (%)	w/c	Slump mm. (in.)	VB Time (sec.)	Air Content (%)
0	0	0.43	152 (6.0)	-----	5.5
0	10	0.32	190 (7.5)	-----	4.5
0.75	0	0.45	127 (5.0)	6.5	6.5
0.75	10	0.34	152 (6.0)	5.0	5.0

--- = no measurement taken
V_f = fiber volume fraction;
L/c= latex-cement ratio, by solids weight;
w/c= water-cement ratio, by weight;
s/c=2.5=sand-cement ratio, by weight; and
st./c=1.5=stone-cement ratio, by weight.

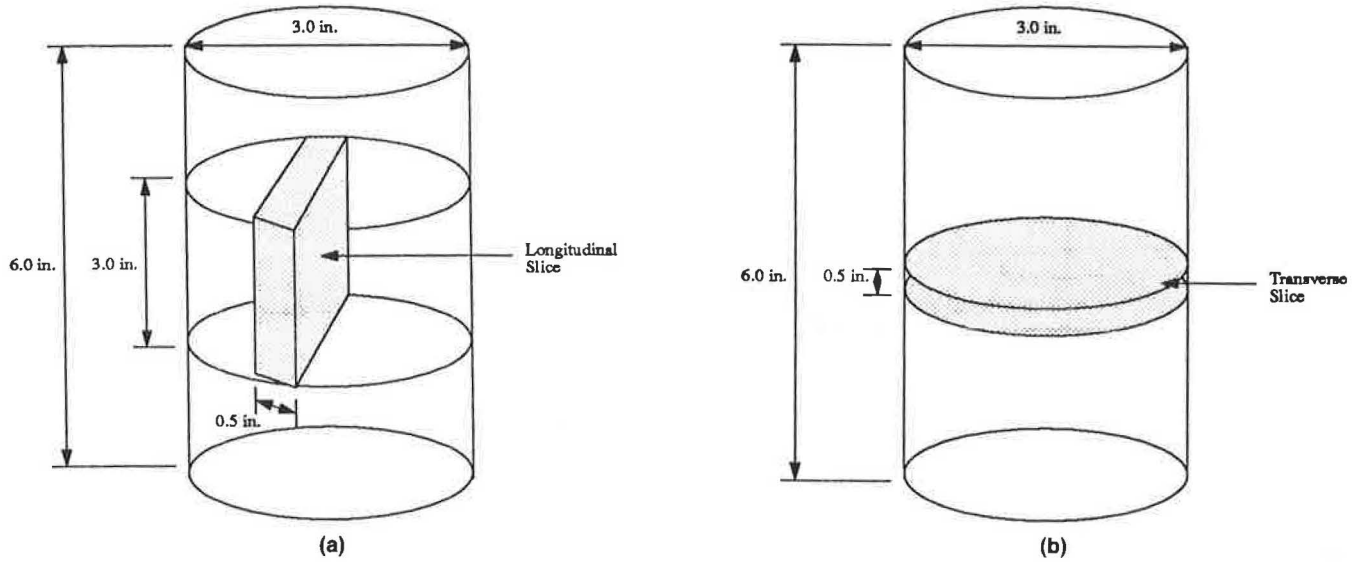

FIGURE 8 Locations of transverse and longitudinal slices, (a) longitudinal slice, and (b) transverse slice.

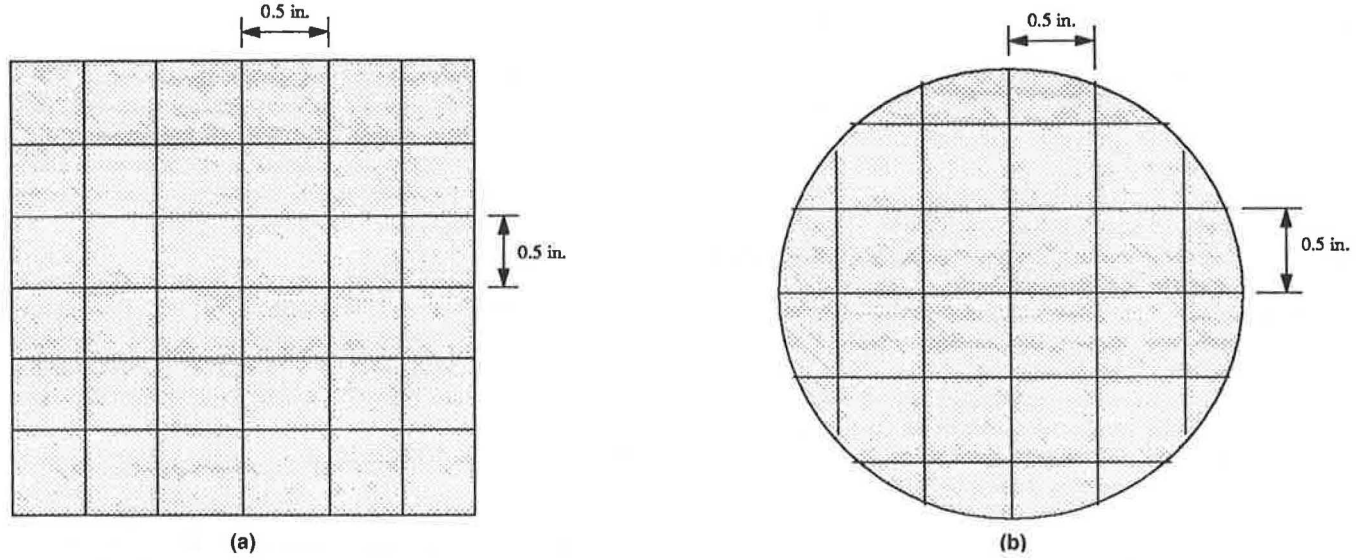

FIGURE 9 Slices ready to be viewed under the microscope, (a) longitudinal slice, and (b) transverse slice.

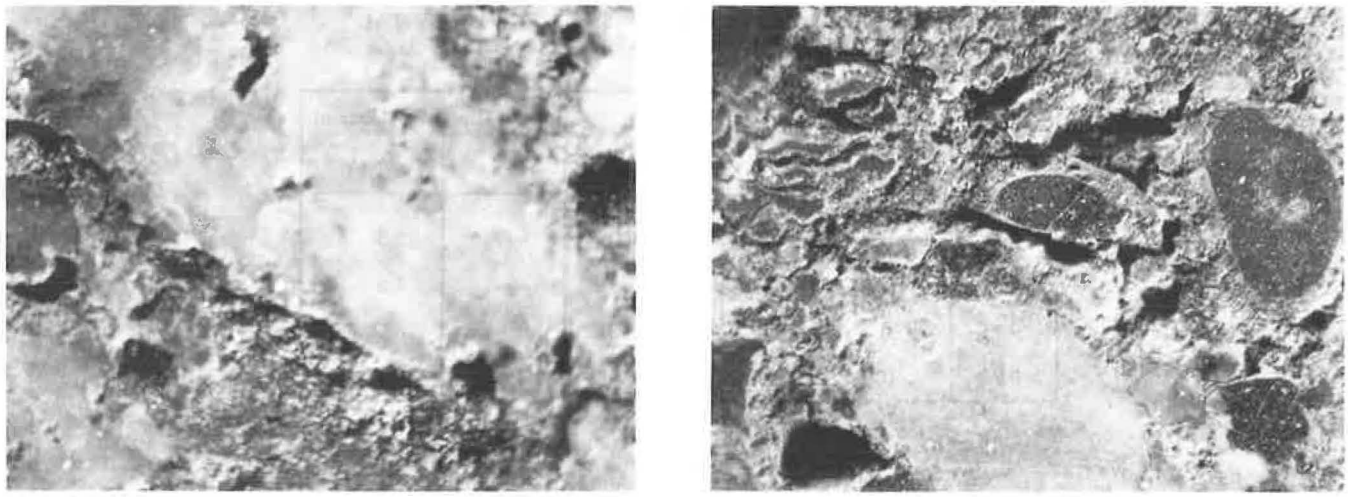

FIGURE 10 Bond cracks at (a) aggregate-cement and (b) fiber-cement interfaces.

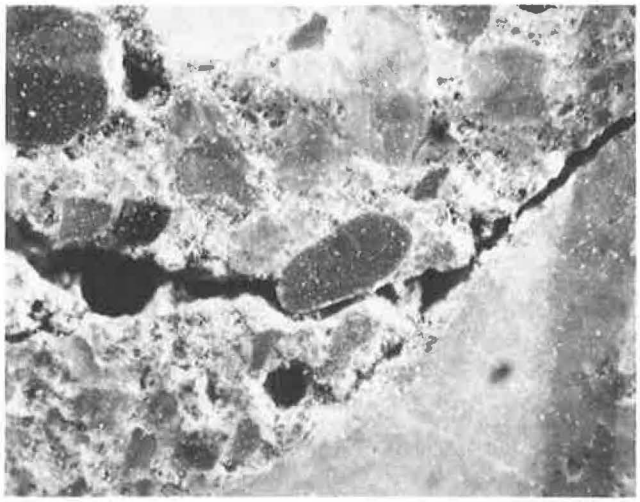

FIGURE 11 Typical matrix microcracks.

fiber-reinforced concrete (LMSFRC) materials are discussed in this section. Conclusions regarding the latex modification and fiber reinforcement effects on the failure mechanism of concrete materials are also presented.

Results of crack intensity (i.e., crack length per unit area of cross section) measurements at different compressive stress levels on plain concrete specimens for transverse and longitudinal sections are shown in Figures 12a and 12b, respectively. The crack intensity at the transverse section is more representative of the actual conditions than that obtained at the longitudinal section. This distinction results from the fact that microcracks tend to propagate in vertical planes. Hence, although a transverse section cuts many of these cracks, the longitudinal section occurs along or in between the approximately vertical crack planes and thus does not present a typical crack intensity.

Microcracks are observed in Figure 12 to be present even before loading (at 0 percent stress level). These microcracks are caused by the differential shrinkage movements, settlements, and thermal strains between aggregates and cement paste, and also by the bleeding effects. They appear dominantly at the interfaces between coarse aggregate and cement paste interfaces (see Figure 12). Similar observations using identical techniques have been made by Shah (*2*). The propagation of these microcracks under compression (which starts to take place mainly at the interfaces and then extends into the matrix as previously shown in Figure 11) is shown quantitatively in Figure 12. At the peak compressive stress, microcracks have a tendency to interconnect and localize, leading to the formation of macrocracks with increasing widths. The process of microcrack propagation takes place at an increasing rate in the postpeak region where microcracks tend to be unstable. Similar observations using identical techniques have been made previously by Shah and Sankar (*2*).

The microcrack intensity in LMC under increasing compressive stresses is shown in Figure 13. Comparison of Figures 12a and 13a, for the more representative transverse sections, indicates that the microcrack intensities tend to be reduced at lower stress levels with latex modification. In particular, microcracks occurring at aggregate-paste interfaces tend to

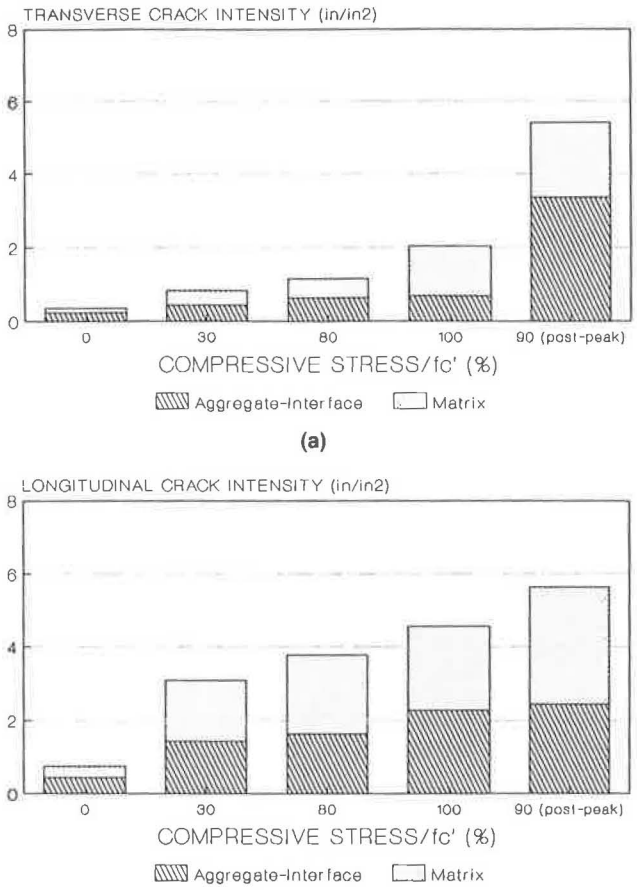

FIGURE 12 Microcrack intensities at different compressive stress levels in plain concrete for (a) transverse section, and (b) longitudinal section.

be reduced substantially in the presence of latex polymers, confirming previous findings (*3*) that latex modification provides improved bonding between the cementitious paste and aggregates. Reduced microcrack intensity in the presence of latex polymers may result from the restraint of microcrack propagation by polymer films bridging across these cracks. In the postpeak region, where the interconnection and localization of microcracks lead to the formation of macrocracks with increasing widths, the failure mechanism in LMC was comparable to that in plain concrete.

The microcrack intensities at different stress levels for SFRC are shown in Figure 14. The appearance of fiber-interface microcracks (see Figure 15), which could be initiated by the same phenomena causing aggregate-interface microcracks, is the new phenomenon that seems to have an unexpected dominant effect in deciding the failure mechanism of SFRC. The formation of fiber-interface microcracks and their relatively rapid propagation (see Figure 16) under increasing compressive stresses in the prepeak region seems to reduce the effectiveness of steel fibers in arresting the propagation of microcracks. In the postpeak region, however, the crack system seems to be more stable in SFRC (Figure 14a) than in plain concrete (Figure 12a) and in LMC (Figure 13a).

Latex modification of SFRC, as shown in Figure 17, seems to stabilize the fiber-interface microcracks under increasing

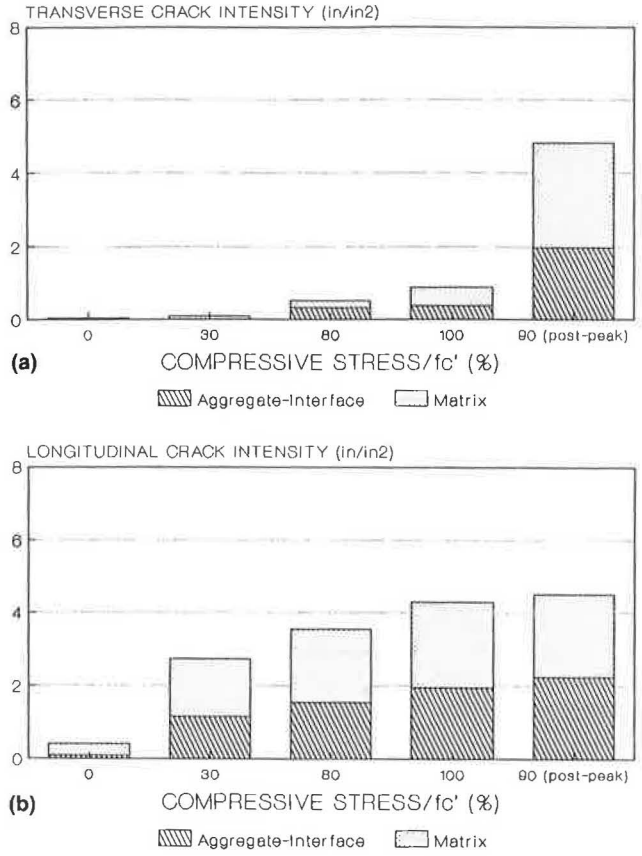

FIGURE 13 Microcrack intensities at different compressive stress levels in LMC, (a) transverse section, and (b) longitudinal section.

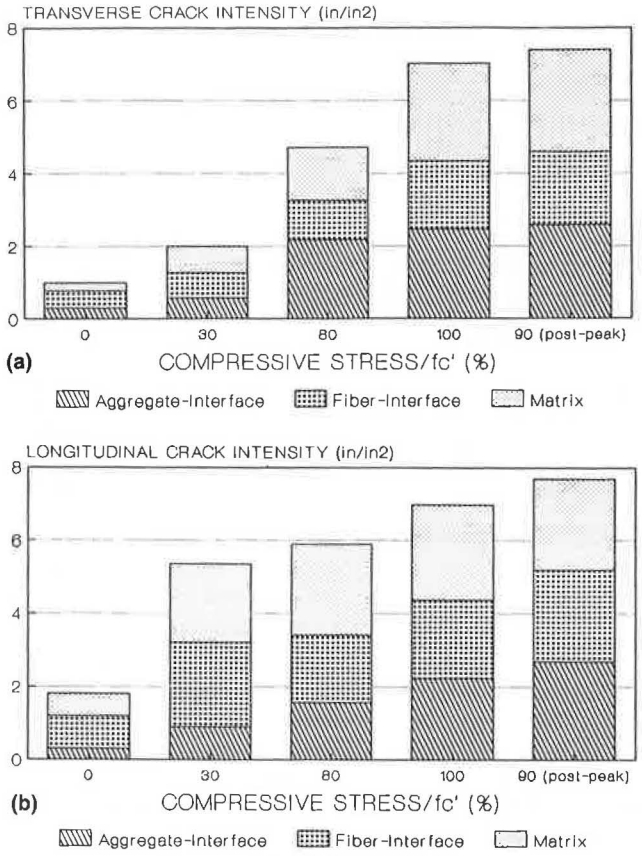

FIGURE 14 Microcrack intensities at different compressive stress levels in SFRC for (a) transverse section, and (b) longitudinal section.

compressive stresses. The aggregate-interface microcracks were also partly controlled by the presence of latex polymers in SFRC. Figure 10 shows these points by showing better fiber- and aggregate-interface bonds even at high compressive stress levels.

The matrix microcrack orientations at the longitudinal sections were generally less than 20 degrees from the longitudinal axis of the specimen (i.e., the loading direction). The microcrack orientation at the aggregate- and fiber-matrix interfaces seemed to be random.

SUMMARY AND CONCLUSIONS

The effects of latex modification and steel reinforcement on the microcracking process of failure mechanism in concrete materials subjected to compression loads were studied. For this purpose, concrete specimens were subjected to different levels of compressive stress in the prepeak and postpeak regions, and were then unloaded. Image analysis techniques were used to quantify microcrack intensities within the paste and at the aggregate- and fiber-matrix interfaces at different load levels. The results indicated that

1. Microcracks are present in concrete materials, dominantly at the coarse aggregate-matrix and fiber-matrix interfaces, even before any loading. These microcracks may be caused by differential shrinkage and thermal movements between cementitious matrices and mix inclusions (i.e., aggregates and fibers);

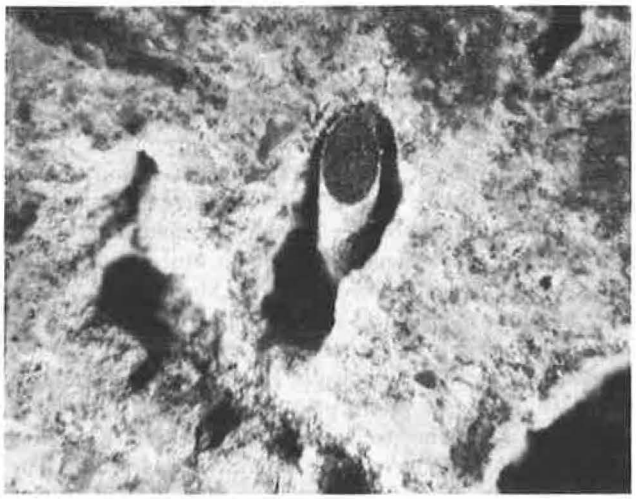

FIGURE 15 Typical fiber interface microcracks.

2. In plain concrete, microcracks tend to originate mainly at the interfaces between coarse aggregate and cement paste,

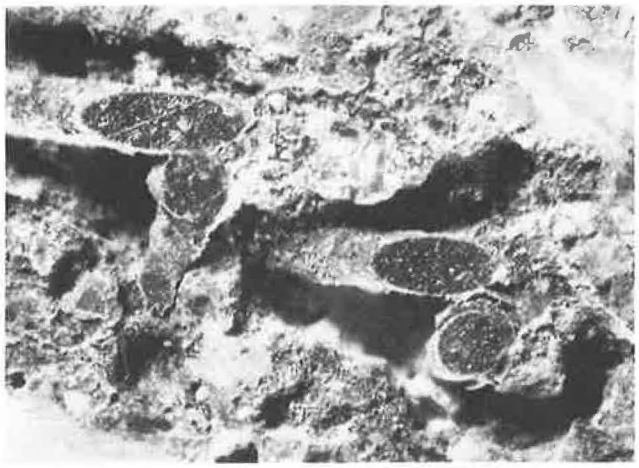

FIGURE 16 Microcracking caused by rapid fiber-interface microcrack propagation.

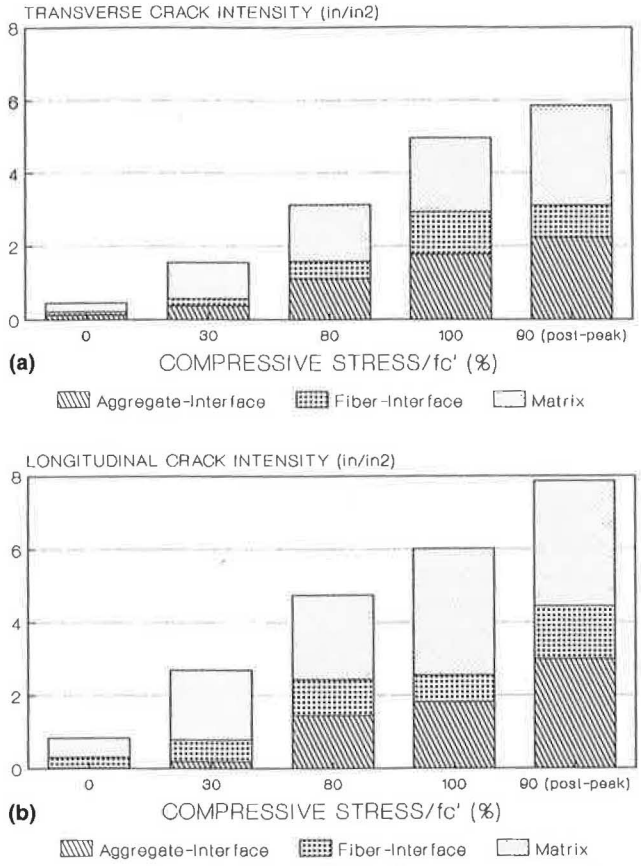

FIGURE 17 Microcrack intensities at different compressive stress levels in LMSFRC for (a) transverse section and (b) longitudinal section.

and then extend into the matrix at higher compression levels; near the peak load, microcracks tend to interconnect and localize, forming macrocracks with increasing widths; there is a rather sudden growth in microcrack intensity beyond the peak compression load;

3. In LMC, the microcrack intensities, especially at aggregate-paste interfaces, tend to be reduced, indicating improvements in bonding between the cementitious paste and aggregates as a result of latex modification; beyond the peak load, however, the sudden increase in microcrack intensity still takes place in spite of latex modification;

4. In unmodified SERC, the fiber-matrix interface microcracks seem to play a dominant role in deciding the failure mechanism of the concrete matrix because of their relatively rapid propagation under increasing compressive stress levels; steel fibers, however, control microcrack propagation in the post-peak region; and

5. Latex modification of SFRC seems to stabilize the fiber-matrix interface microcracks as well as the aggregate-matrix interface microcracks leading to a more stable microcrack system within SFRC materials.

ACKNOWLEDGMENTS

Financial support for the performance of this research was provided by BASF Canada, Inc., and the Research Excellence Fund of the State of Michigan. These contributions are gratefully acknowledged. The authors are also thankful to Kar Lok of BASF Canada, Inc., and Lawrence T. Drzal of the Composite Materials and Structures Center, Michigan State University, for their encouragement and technical support.

REFERENCES

1. S. P. Shah. *Application of Fracture Mechanics to Cementitious Composites.* Advanced Science Institute Series E, Martinus Nijhoff Publishers, Boston, Mass., 1985.
2. S. P. Shah and R. Sankar. Internal Cracking and Strain-Softening Response of Concrete Under Uniaxial Compression. *ACI Materials Journal*, American Concrete Institute, Detroit, Mich., May–June, 1987, pp. 200–212.
3. J. E. Isenberg, D. E. Rapp, E. J. Sutton, and J. W. Vanderhoff. *Microstructure and Strength of the Bond Between Concrete and Styrene-Butadiene Latex-Modified Mortar.* In *Highway Research Record 370*, TRB, National Research Council, Washington, D.C., 1971, pp. 75–89.

Publication of this paper sponsored by Committee on Mechanical Properties of Concrete.